Modeling of combustion in engines fed by hydrogen

Nickolay Smirnov[1,2], Yurii Phylippov [2], Valeriy Nikitin[1,2], Mikhail Silnikov[3],

[1] Scientific Research Institute for System Analysis of the Russian Academy of Sciences,
36-1 Nakhimovskiy pr., Moscow 117218,
RUSSIA
[2]Moscow M.V. Lomonosov State University,
Leninskie Gory, 1, Moscow 119992,
RUSSIA,
[3] Saint Petersburg State Polytechnical University,
29 Politechnicheskaya Str., 195251 St. Petersburg
RUSSIA

ebifsun1@mech.math.msu.su

Abstract: - Computer aided design of new effective and clean hydrogen engines needs mathematical tools for supercomputer modeling of hydrogen – oxygen components mixing and combustion in rocket or aviation engines.

The paper presents the results of developing verification and validation of mathematical model making it possible to simulate unsteady processes of ignition and combustion in RAM or pulse detonation engines.

One of peculiarities of hydrogen-oxygen rocket engine is the following. On injecting liquid components fuel (hydrogen) having must lower critical temperature comes pre-evaporated and pre-heated in combustion chamber, while oxygen could be liquid then evaporating inside the chamber. Thus contrary to most types of engines hydrogen engine has an inverse mixture entering combustion chamber, in which fuel is gaseous and oxidant is liquid.

Onset of detonation being very dangerous for classical RAM engines could, however, serve the basis for creating new generation of engines - pulse detonating engines (PDE). For this issue the problems of detonation onset and deflagration to detonation transition should be simulated quite accurately, because these processes strongly depend on inlet conditions, mixture composition and geometrical characteristics of combustion chamber.

Key-Words: - Combustion, ignition delay, non-equilibrium, diffusion, turbulence, mathematical simulation

1 Introduction[´]

Rocket engines using hydrogen-oxygen mixture have the following peculiarity. On injecting liquid components fuel (hydrogen) having much lower critical temperature comes pre-evaporated and pre-heated in combustion chamber, while oxygen could be liquid then evaporating inside the chamber. Thus contrary to most types of engines hydrogen engine has an inverse mixture entering combustion chamber, in which fuel is gaseous and oxidant is liquid. However, taking into account rather low critical temperatures for both components estimates based on models developed in [1-3] show, that phase transition will take place in an order of magnitude faster then for hydrocarbon fuels. That provides the reason to use one phase model as a first order of approximation. Onset of detonation being very dangerous for classical RAM engines could, however, serve the basis for creating new generation of engines - pulse detonating engines (PDE) [4]. For this issue the problems of flame stabilization [5] and detonation onset, decay and deflagration to detonation transition should be simulated quite accurately, because these processes strongly depend on inlet conditions,

[´] Russian Foundation for Basic Research (RFBR 13-03-00003) and Presidium of RAS (Program 18) are acknowledged for financial support.

mixture composition and geometrical characteristics of combustion chamber [6-8].

Hydrogen chemistry modeling is rather complicated because regular kinetic mechanisms have hundreds stages. Many reduced kinetic mechanisms were developed. However, peculiarities of hydrogen combustion kinetics, the presence of zones of inverse dependence of reaction rate on pressure, makes developing reduced mechanisms a very difficult task, which was studied by many researchers [9-13]. In the present paper kinetic models developed based on methodology [15] will be used. The validation of these models will be performed based on experimental investigations of ignition delay times being functions of pressure, temperature and mixture composition [16].

Combustion in terrestrial conditions is strongly affected by thermogravitational instability, which provides additional very effective mixing of the components and formation of combustible mixture in the vicinity of each droplet. On the contrary, this mechanism does not work under low gravity conditions. Only diffusion contributes to mixing, which makes ignition and combustion conditions less favorable.

It should be mentioned, that thermo-convective effect on droplet evaporation manifest as long as Mar number is larger then unity $\mathrm{Mar} = t_{evap} / t_{conv} > 1$. This number for evaporating droplet could be evaluated as $\mathrm{Mar} = t_{evap} / t_{conv} = \dfrac{\sqrt{g r_0^3} h_L}{D c_{pe} (T_e - T_W)}$.[3] Under microgravity conditions Mar number tends to zero and thermo-convective mixing is not essential for all sizes of droplets. Thus ignition and combustion under microgravity needs special accounting for microgravity diffusive combustion modes [14, 17].

2 Mathematical model

Numerical investigations of the DDT processes were performed using the system of equations for the gaseous phase obtained by Favre averaging of the system of equations for multicomponent multiphase media. The modified *k-epsilon* model was used. To model temperature fluctuations the third equation was added to the *k-epsilon* model to determine the mean squared deviate of temperature [7, 8]. The production and kinetic terms were modeled using the Gaussian techniques [18, 19].

The gaseous phase was supposed to contain the following set of species: $\{H_2O, OH, H, O, HO_2, H_2O_2; O_2, H_2, N_2\}$.

The following brutto reactions between the species were considered:

N_R	**Reaction**	**Reaction rate coefficient** k_r^D
1.	$O_2 + H \Leftrightarrow OH + O$	$2.00 \cdot 10^{14} \cdot \exp\left[-70.3 / R_G T\right]$
2.	$H_2 + O \Leftrightarrow OH + H$	$5.06 \cdot 10^{4} \cdot T^{2.67} \cdot \exp\left[-26.3 / R_G T\right]$
3.	$H_2 + OH \Leftrightarrow H_2O + H$	$1.00 \cdot 10^{8} \cdot T^{1.60} \cdot \exp\left[-13.8 / R_G T\right]$
4.	$OH + OH \Leftrightarrow H_2O + O$	$1.50 \cdot 10^{9} \cdot T^{1.14} \cdot \exp\left[-0.4 / R_G T\right]$
5.	$H + H + M \Leftrightarrow H_2 + M$	$1.80 \cdot 10^{18} \cdot T^{-1.00}$
6.	$+O + M \Leftrightarrow O_2 + M$	$2.90 \cdot 10^{17} \cdot T^{-1.00}$
7.	$H + OH + M \Leftrightarrow H_2O + M$	$2.20 \cdot 10^{22} \cdot T^{-2.00}$
8.	$H + O_2 + M \Leftrightarrow HO_2 M$	$2.30 \cdot 10^{18} \cdot T^{-0.80}$
9.	$HO_2 + H \Leftrightarrow OH + OH$	$1.50 \cdot 10^{14} \cdot \exp\left[-4.2 / R_G T\right]$
10.	$HO_2 + H \Leftrightarrow H_2 + O_2$	$2.50 \cdot 10^{13} \cdot \exp\left[-2.9 / R_G T\right]$
11.	$HO_2 + H \Leftrightarrow H_2O O$	$3.00 \cdot 10^{13} \cdot \exp\left[-7.2 / R_G T\right]$
12.	$HO_2 + O \Leftrightarrow OH + O_2$	$1.80 \cdot 10^{13} \cdot \exp\left[+1.7 / R_G T\right]$
13.	$HO_2 + OH \Leftrightarrow H_2O + O_2$	$6.00 \cdot 10^{13}$
14.	$HO_2 + HO_2 \Leftrightarrow H_2O_2 + O_2$	$2.50 \cdot 10^{11} \cdot \exp\left[+5.2 / R_G T\right]$
15.	$OH + OH + M \Leftrightarrow H_2O_2 + M$	$3.25 \cdot 10^{22} \cdot T^{-2.00}$
16.	$H_2O_2 + H \Leftrightarrow H_2 + HO_2$	$1.70 \cdot 10^{12} \cdot \exp\left[-15.7 / R_G T\right]$

17.	$H_2O_2 + H \Leftrightarrow H_2O + OH$	$1.00 \cdot 10^{13} \cdot \exp\left[-15.0 / R_G T\right]$
18.	$H_2O_2 + O \Leftrightarrow OH + HO_2$	$2.80 \cdot 10^{13} \cdot \exp\left[-26.8 / R_G T\right]$
19.	$H_2O_2 + OH \Leftrightarrow H_2O + HO_2$	$5.40 \cdot 10^{12} \cdot \exp\left[-4.2 / R_G T\right]$

Table 1. Kinetic mechanism [12]

In table 1 reactions 1 – 4 correspond to reaction exchanges involving "light" radicals O, H, OH, reactions 5 – 7 are responsible for recombination of "light" radicals, in reactions 8 – 13 "heavy" radical HO_2 is involved as well, the rest of reactions 14 – 19 are characterized by the presence of another "heavy" radical H_2O_2.

Mechanism [12] assumes the effect of third body in recombination reactions to be described by one and the same coefficient for all reactions. The coefficients are present in the table 2. For all other components not present in the table Chaperon coefficients are assumed to be unity.

	H2	O2	H2O	N2
γ_k	1.0	0.4	6.5	0.4

Table 2. Chaperon coefficients for reduced reaction mechanism presented in table 1.

3 Combustion chamber with coaxial injection of oxygen and hydrogen

Diffusion combustion onset in a model combustion chamber [5] was simulated numerically using Logos code [19, 35]. Oxygen was delivered through the inner nozzle, hydrogen was delivered through the ring surrounding nozzle.

Simulations were performed for the following model parameters.

Unsteady-state simulation regime incorporating 10 iterations per time step. Explicit scheme with constant Courant number 0.15. Turbulence model SA (Spalart – Allmaras). Scheme TVD is used for solving gas dynamic equations. Computational domain has an axial symmetry. The model chamber is initially filled in with nitrogen, pressure $P_{ini} = 1$ бар, temperature $T_{ini} = 300$ К, velocity equals to zero. Through central inlet nozzle (surface IN1) cool oxygen is delivered. Through peripheric ring inlet (surface IN2) heated hydrogen is delivered. Inlet velocity is parallel to axis of symmetry. The inlet data values are present in the table 3. The outlet condition on the right hand side is constant pressure $P_{out} = 1$ bar. No slip conditions were placed on all walls.

IN1			IN2		
P_{stat}, бар	P_{tot}, бар	T_{tot}, К	P_{stat}, бар	P_{tot}, бар	T_{tot}, К
2.5	2.7	250	3.0	3.2	1300

Table 3. Inlet conditions. P_{stat} -static pressure, P_{tot} -total pressure (static+dynamic), T_{tot} -stagnation temperature.

The chamber was initially filled in with nitrogen. Fig. 1 shows successive stages of chamber flow until it reaches stable combustion regime.

$t = 0.1$ ms

$t = 0.2$ ms

$t = 0.3$ ms

$t = 0.4$ ms

$t = 0.5$ ms

Fig. 1. Dynamics of pressure (left) and axial velocity (right) stabilization after launching the combustion chamber.

$t = 0.8$ ms

$t = 1.0$ ms

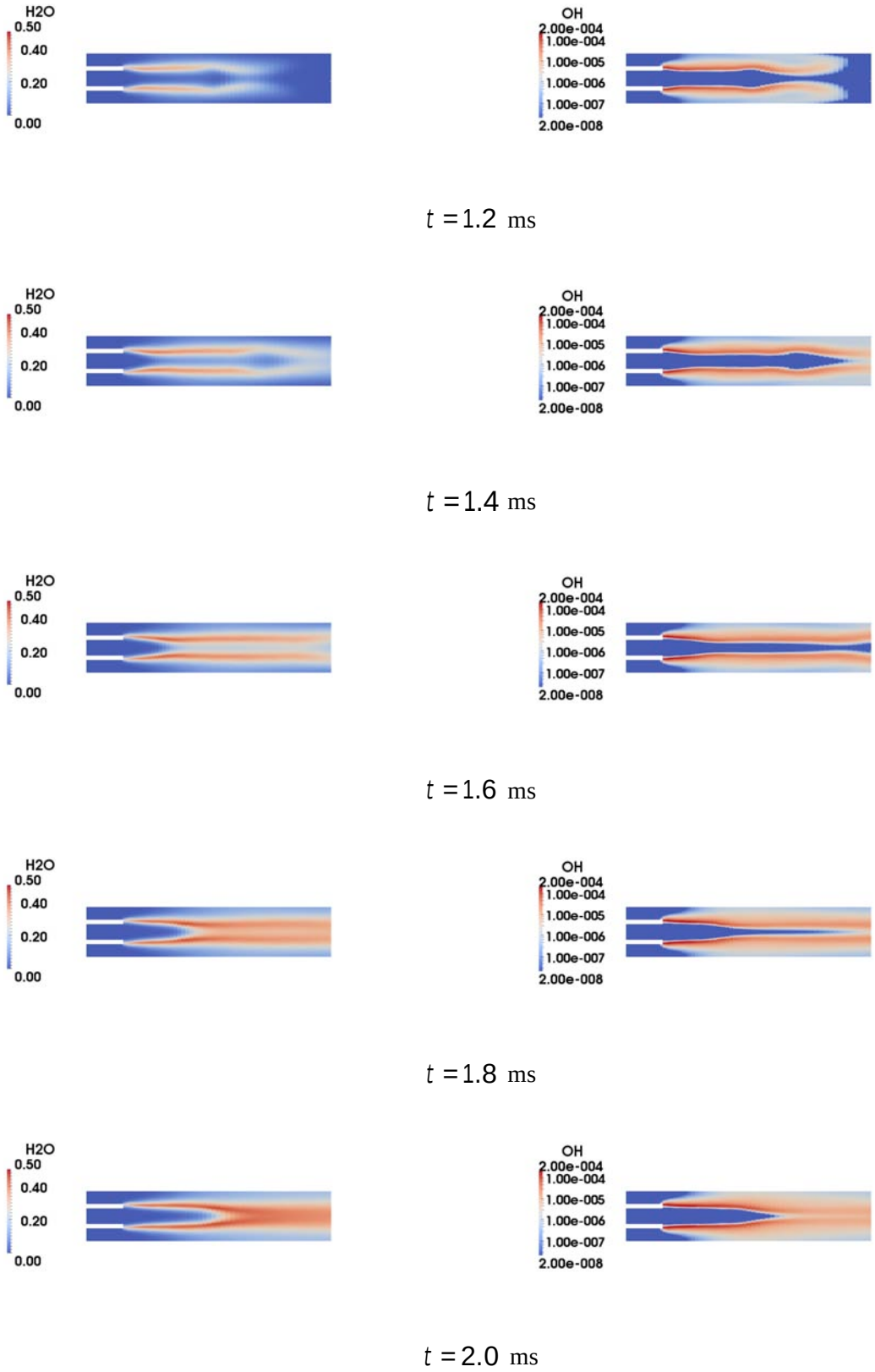

Fig. 2. Dynamics of water vapor concentration (reaction product, left) OH radical (right) stabilization after launching the combustion chamber.

As it is seen from Figs. 1 and 2 before establishing steady-state combustion regime in the chamber strong pressure and velocity oscillations take place caused by shock waves propagation both in longitudinal and transverse directions. But stabilization of gas dynamic parameters (pressure and velocity) comes faster then stabilization of reaction zone. In stable regime pressure monotonously decreases from inlet to the outlet. Axial velocity increases. Dynamics of OH

radical concentration helps us to trace the flame zone, because peculiarity of hydrogen combustion mechanism makes this radical formation and death take place within the flame zone. It is an intermediate product. (Fig. 2). Analysis of species concentrations distribution shows that diffusion combustion regime was established near the nozzle. Narrow zone of OH radical presence testifies that. Diffusion combustion regime is characterized by very fast chemical reactions surpassing the rate of diffusion transport of species to reaction zone. Under these conditions reagents are unable to penetrate deep through the mixing zone not entering into chemical reaction. The zone of reaction conversion is very narrow, and the process is governed by diffusion rather than chemistry. However, on moving away from the nozzle the mixing zone becomes wider and concentration gradients decrease. But along with this decrease of reagent concentration takes place, which brings to a decrease of chemical reaction rate and increase of induction time. Thus chemical reaction becomes limiting factor and reaction rate begins to play important role as compared with diffusion. Under this condition reaction zone becomes wider and occupies the whole chamber. But reaction intensity is much lower, which is shown by the decrease of OH radical concentration. The situation is due to mixture being enriched: the system runs out of oxygen earlier than hydrogen is consumed thus coming to long ignition delay times. The reaction product – water vapor – distribution in Fig. 2 shows, that conversion of hydrogen was not complete, because there are no reaction products found near the wall. The conclusion, which one could drive out of this model simulation, should be that initial inlet parameters were sufficient for establishing stable combustion in the chamber, but not optimal to guarantee maximal conversion of reagents within the combustion chamber domain. The developed numerical tool makes it possible to perform optimization studies for hydrogen – oxygen combustion chambers.

Fig. 3 illustrates an experimental one-injector chamber of SSME type [http://ntrs.nasa.gov/] and numerical grid used in simulations by Logos code [35].

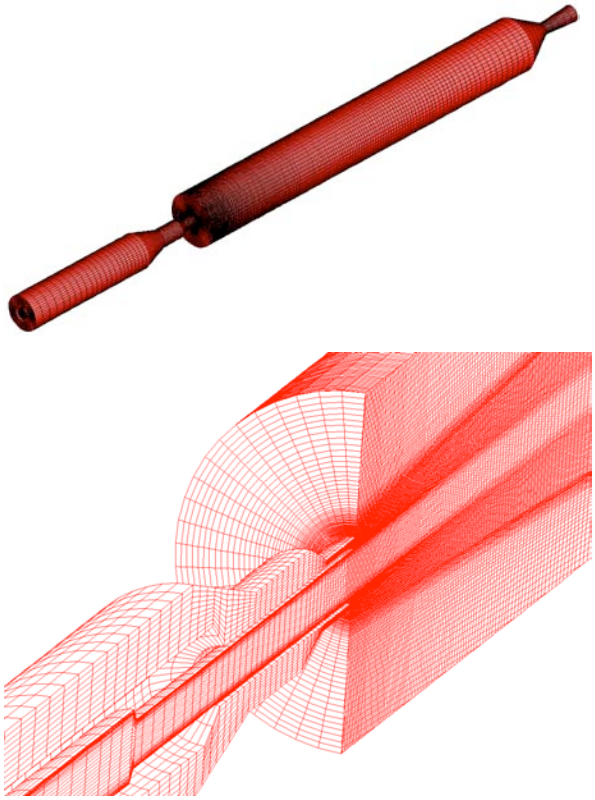

Fig.3. Experimental combustion chamber and grid details.

Results of numerical simulations are present in Fig. 4 in the form of maps of different flow parameters in the axial cross-section.

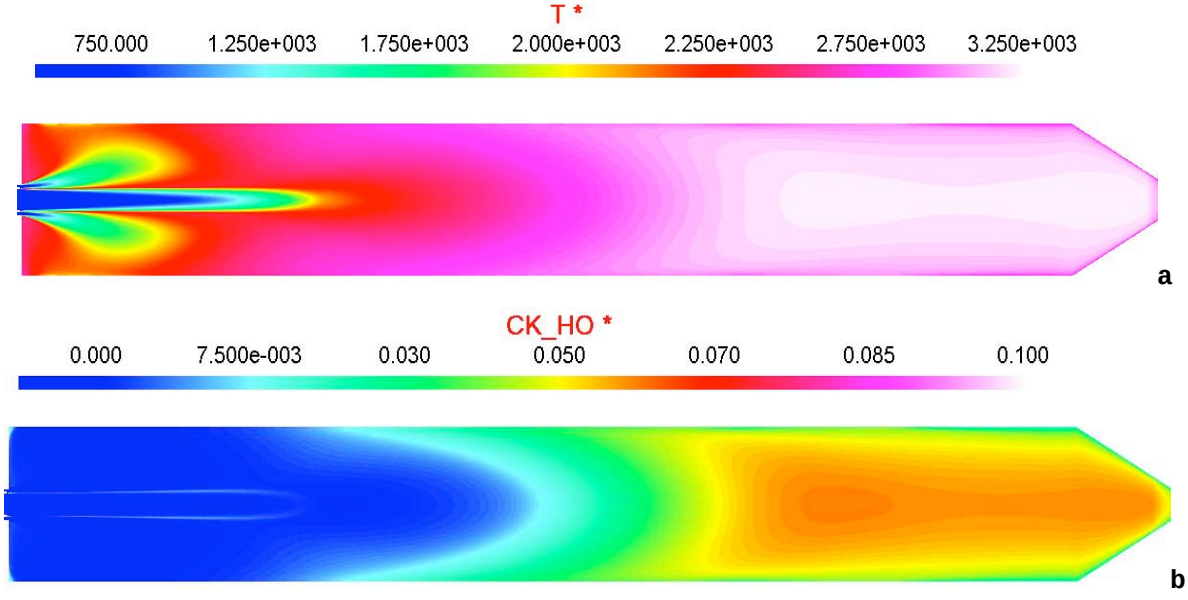

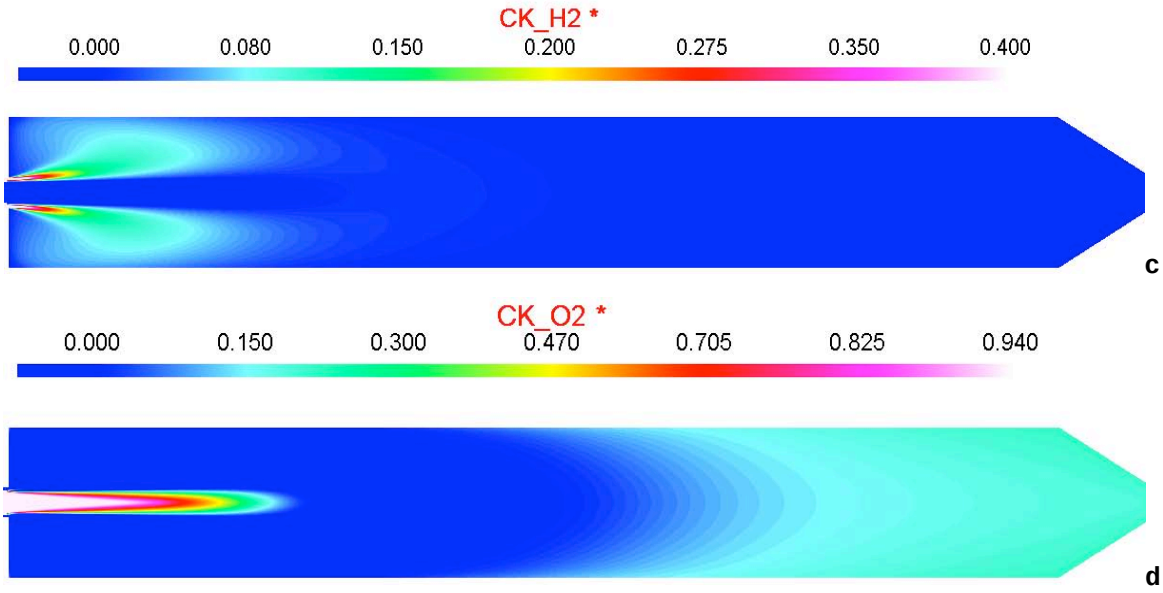

Fig. 4. Flow parameters maps in axial cross-section of model combustion chamber: a – tempersture, b – OH radical mass concentration, c – hydrogen mass concentration, d – oxygen mass concentration.

4 Detonation decay and re-initiation on entering wider chamber

The control of detonation onset in large chambers is of major importance in pulse detonating devices. The advantages of detonation mode of energy conversion over constant pressure combustion bring to the necessity of promoting the onset of detonation and shortening the pre-detonation length. The onset of detonation in large chambers could be promoted in two ways.

First way is promoting DDT in the whole chamber using different turbulizing elements, such as Schelkin spiral, orifice plates, or wider cavities [4]. The method is very effective, mostly using wider cavities [5], but the predetonation length turns to be big for wide chambers [8].

Second way is promoting onset of detonation in narrow chambers, which needs much shorter pre-detonation length, and then transmitting the detonation to a wider chamber. The method is effective in terms of shortening the predetonation length, but there is a great probability the transmission of detonation could fail under certain conditions.

Detonation wave can be transmitted in a wider chamber from a narrow peripheric coaxial gap. On entering wider chamber decay of detonation wave begins due to divergence and decay of transverse waves. But cumulative effect on converging waves the center of the cylinder makes leading shock wave stronger, which promotes re-initiation of detonation. Of course, all scenarios are strongly dependent on reaction rate, which means on mixture composition and mixture temperature. Below Figs. 5 illustrate transmission of a detonation wave from a narrow gap 20 mm width into a big cylindrical chamber 200 mm diameter. The upper part of each figure illustrates pressure fields in a cross-section, the lower part illustrates temperature fields, as the model problem was assumed to have axial symmetry.

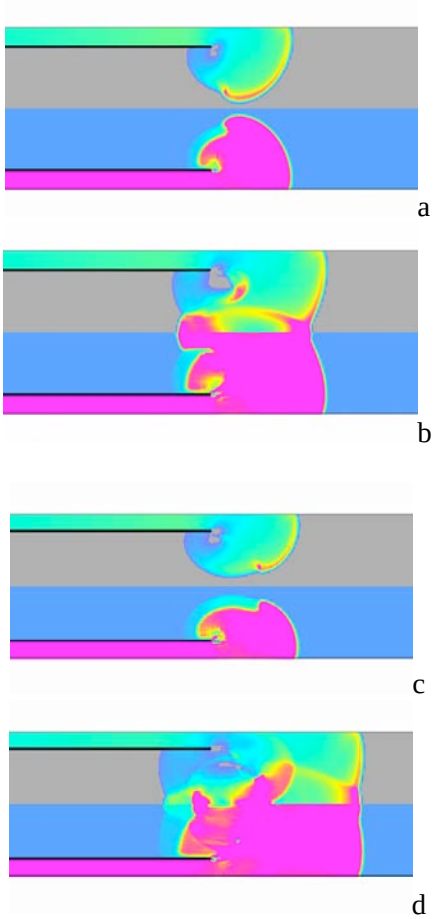

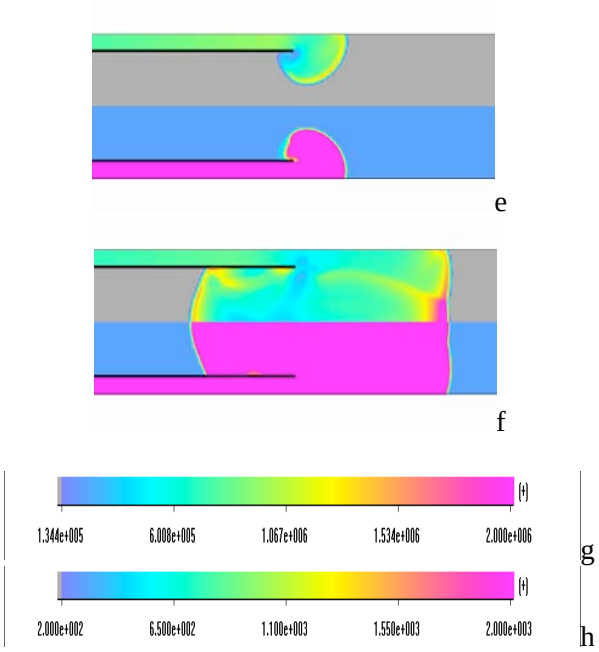

Fig. 5. Transmitting detonation wave from narrow gap to cylindrical chamber : a,b - $H_2 : O_2 : N_2 = 1{,}5 : 1 : 5$; c,d - $H_2 : O_2 : N_2 = 2 : 1 : 7$; e,f - $H_2 : O_2 : N_2 = 2 : 1 : 5$; mapping scales for pressure (g) and temperature (h).

As it is seen from the figures, transmission of detonation finally succeeds in all cases, but the fastest process takes place in a stoicheometric hydrogen – air mixture (Fig. 5), which is coherent to theoretical models, because stoicheometric hydrogen – air mixtures have the shortest ignition delay time (Fig. 3), which means faster reaction rate and smaller detonation cell size. However, for lean mixture (Fig. 3) and diluted stoicheometric mixture (Fig. 4) transmission of detonation is also successful for the present configuration, while direct transmission from 20 mm diameter tube into 200 mm diameter tube fails for both lean and diluted mixture. As it is seen from Figs. 13 and 14, on entering wider chamber from a narrow gap reaction front lags behind the leading shock due to the effect of front stretch. Transverse waves travel only in the direction of expansion, because there are no reflected waves traveling from that side. It can be clearly traced from temperature maps, because temperature behind the transverse detonation wave increases close to its equilibrium value. Then convergence of shock waves to the axis of symmetry of the cylinder brings to an increase of its intensity and reinitiation of detonation upon reflection from the axis. Fig. 6 illustrates more stages of transmission of a detonation wave in diluted stoicheometric mixture, which makes it possible to trace the mechanism of degeneration and reestablishing of detonation wave.

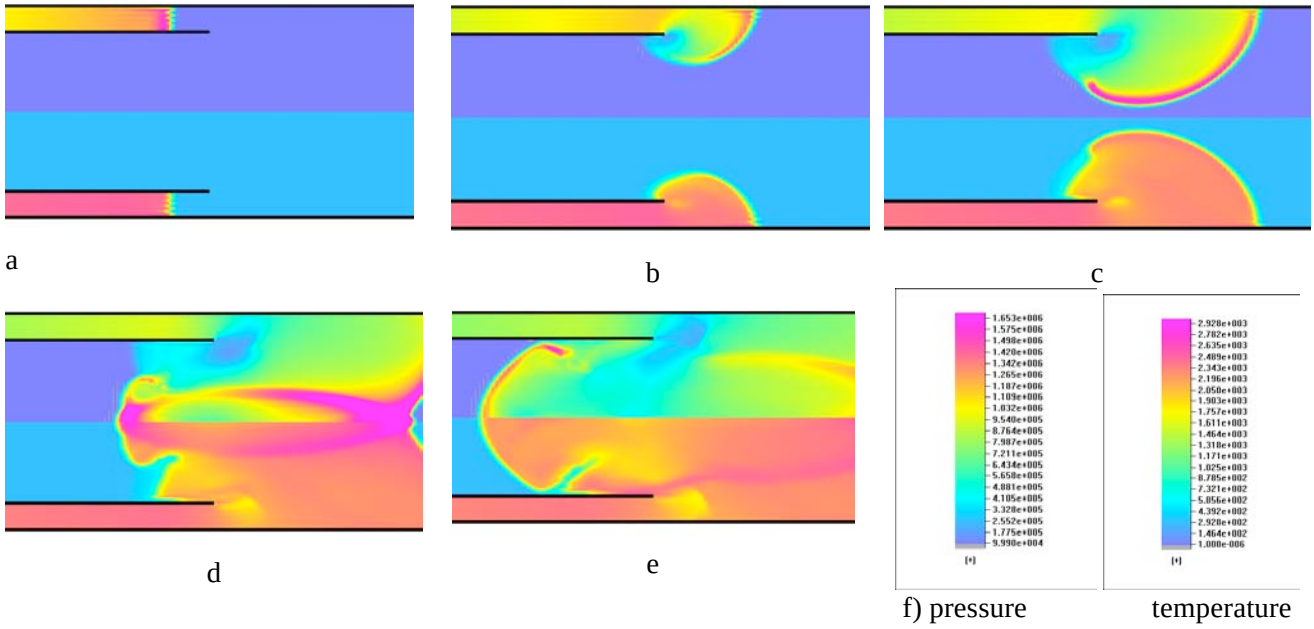

Fig. 6. Transmitting detonation wave from narrow gap to cylindrical chamber $H_2 : O_2 : N_2 = 2 : 1 : 6$. Times: a - 0.2448 ms, b - 0.2629 ms, c – 0.2707 ms, d - 0.2855 ms, e - 0.2978 ms, f - mapping scales for pressure and temperature.

The result drives us to conclusions, that the suggested configuration is optimal for transmission detonation from narrow to wide chambers, and that developed numerical tool makes it possible to perform optimization studies of hydrogen – oxygen detonation engine design.

5 Deflagration to detonation transition (DDT)

Among all the phenomena relative to combustion processes deflagration to detonation transition is, undoubtedly, the most intriguing one. Deflagration to detonation transition (DDT) in gases is relevant to gas and vapor explosion safety issues. Knowing mechanisms of detonation onset control is of major importance for creating effective mitigation measures addressing the two major goals: to prevent the DDT in case of mixture ignition, or to arrest the detonation wave in case it was initiated. The new impetus to the increase of interest in deflagration to detonation transition (DDT) processes was given by the recent development of pulse detonation devices. The probable application of these principles to creating the new generation of engines put the problem of pulse detonating devices (PDD) effectiveness on top of current research needs. The effectiveness of the PDD cycle turned to be the key factor characterizing the Pulse Detonation Engine (PDE), which operation modes were shown to be closely related to periodical onset and degeneration of a detonation wave. Those unsteady-state regimes should be self-sustained to guarantee a reliable operation of devices using the detonation mode of burning fuels as a constitutive part of their working cycle. Thus deflagration to detonation transition processes are of major importance for the issue. Minimizing the pre-detonation length and ensuring stability of the onset of detonation enables to increase effectiveness of PDD. The DDT turned to be the key factor characterizing the PDE operating cycle. Thus, the problem of DDT control in gaseous fuel-air mixtures became very acute.

The study of DDT in hydrogen-air mixtures,[20-23] and then in hydrocarbon-air mixtures[24, 25] have shown that there are numerous DDT scenarios. Different mechanisms of the detonation initiation depend on a particular flow structure generated by the accelerating flame, and for this reason, all details of the DDT process cannot be reproduced in experiments. Currently, there are different viewpoints on the DDT mechanism: "explosion in an explosion" by Oppenheim [20] and gradient mechanism of "spontaneous combustion" by Zeldovich [26]. Oppenheim observed spontaneous local explosions that were primary sources of the unburned gas layers compression, so that they “exploded” subsequently. Zeldovich suggested the “spontaneous” mechanism according to which combustion wave velocity is determined by gradient of ignition induction time due to non-uniform heating of different unburned gas layers.

A subsequent theoretical analysis showed that a microscale increase in nonuniformity of the temperature distribution and an increase in concentration gradient near local exothermal centers ("hot spots") ahead of the flame front may turn out to be sufficient for an individual hot spot to develop either into a normal combustion wave, or to a detonation wave [27-30]. Oppenheim thought one needed a stochastic modeling of isolated hot spots because their origination and evolution was not understood at the time. However, subsequent modelers used entirely deterministic methods to identify the properties of hot spots and reasons for their origination. An analysis of theoretical and experimental results shows that self-ignition at one or several hot spots ahead of the accelerating flame with subsequent development of combustion or detonation wave from each local exothermal center is responsible for the existence of numerous DDT scenarios [5]. Shock waves arise owing to initiation and influence of the flame as an accelerating spherical piston. Reflection of compression waves from the container walls or from interfaces between gas mixtures of different densities leads to circulation of waves whose amplitude may increase owing to interaction with the flame. The common feature of all these scenarios is the formation of local exothermal centers by Oppenheim’s stochastic mechanism with the subsequent development of detonation at the microscale according to Zeldovich’s spontaneous mechanism [5, 32]. The DDT study in the case of interaction of a reflected shock wave with the laminar flame [31, 32] also shows that the deflagration-to-detonation transition at the hot spots follows the gradient mechanism, whereas the interaction between the shock wave and the combustion wave, as well as local inhomogeneities of the flow, create conditions for the emergence of hot spots themselves. Other investigators explain the detonation wave onset not by spontaneous flame acceleration within a single exothermic center, but rather restructuring of flow being the result of flame interaction with the zone of elevated temperature ahead, which leads in the long run to ignition delay gradients formation sufficient for spontaneous detonation onset [33]. There is no experimental evidence by nowadays that DDT could take place in an open space without any obstacles and wave reflections, nor has anybody obtained such a DDT in numerical simulations [34].

The present study was aimed at adjusting the code for numerical simulation of the whole problem of mild ignition, slow flame onset, flame acceleration and turbulization, and finally deflagration to detonation transition [36-41].

Fig. 7 illustrates the successive stages of the detonation onset in a tube 600 mm long and 20 mm diameter after mild ignition in the left hand side. The upper part of the tube is used for illustrating pressure maps, the lower part (below axis) shows temperature

maps. The mapping colours for pressure and temperature are present in the bottom of Fig. 7 as well. The characteristic times, for which the plots are shown, are depicted in the right hand side of the figure in seconds.

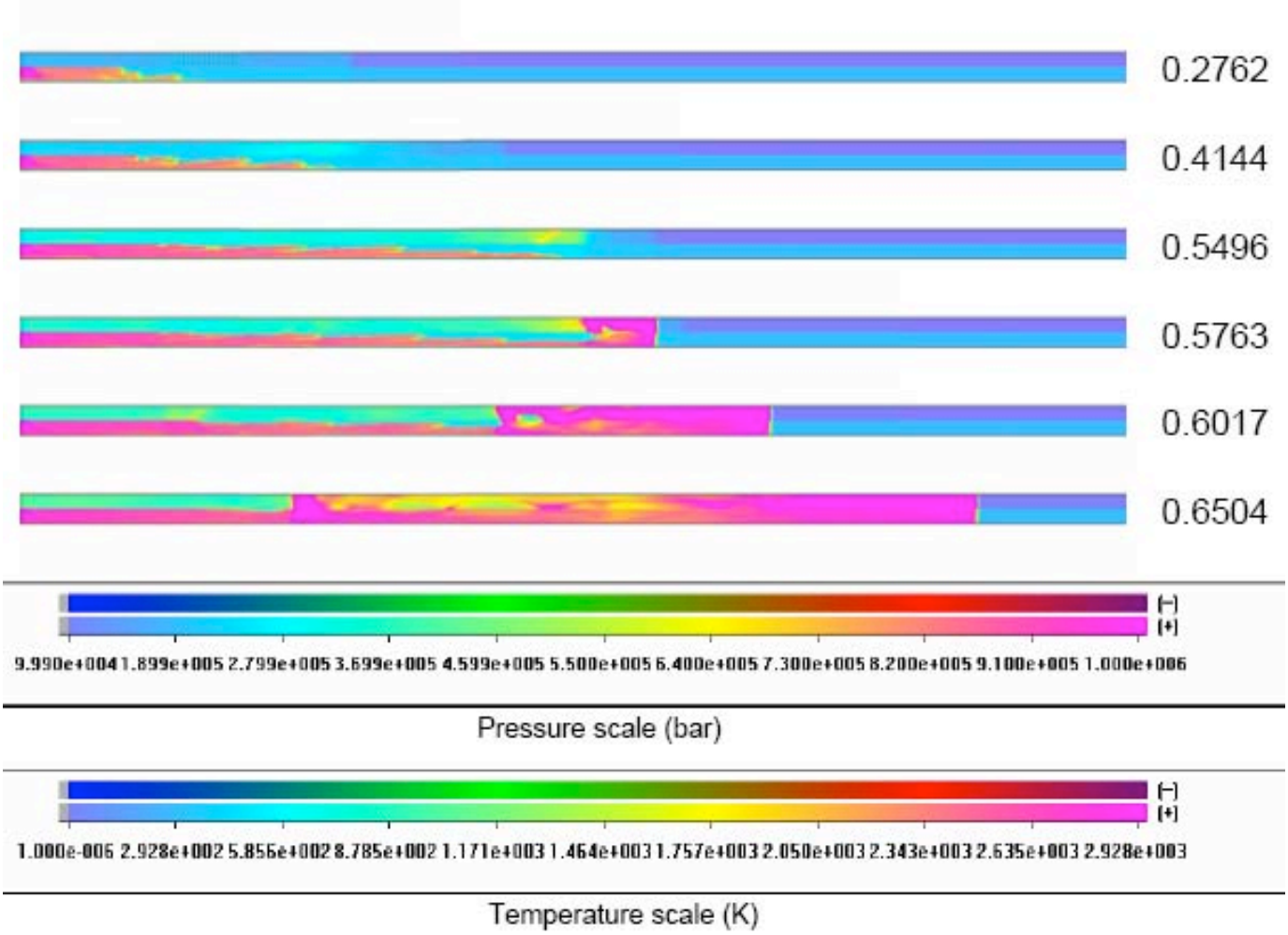

Fig. 7. Successive stages of the detonation onset in a tube 600 mm long and 20 mm diameter after mild ignition in the left hand side in hydrogen – air mixture $H_2 : O_2 : N_2 = 2:1:4$. The upper part of the tube is used for illustrating pressure maps, the lower part (below axis) shows temperature maps.

The tube being relatively long the maps are shown in Fig. 8 in a different scale for the 100 mm sections of the tube for different times. Mapping colors arethe same as shown in Fig. 7.As it is seen from Figure 17, flame propagation begins from the left hand side, which is testified by temperature increase up to the highest value corresponding to the equilibrium state of reaction products. The pressure increase is very small, however, it could be trace on the upper parts of figures for early time moments. For time 0.27 and 0.41 s shock wave in the gas propagates far ahead of the flame front. Then turbulization of the mixture brings to an increase of flame propagation velocity, and the distance between flame zone and leading disturbance shortens. Temperature maps illustrate strong non-uniformity of temperature distribution along tube radius. It is seen that flame propagates faster in the vicinity of the wall, where turbulence is stronger. Finally at t=0.55 s convergence of shock waves brings to pressure increase in the wall zone, which in the long run brings to formation of detonation and retonation waves propagating in the opposite directions. The DDT scenario and the maps are qualitatively similar to those obtained in experiments [20]. The onset of detonation wave in the wall boundary layer zone coincides with theoretical conclusions [27, 28]. More detailed examination of detonation onset zone (Fig. 8 c, d, e) shows that there exist strong transverse shock waves in this zone. Retonation wave propagates backward both in heated reaction products in periphery and cool combustible mixture, however, shock wave in heated products overtakes detonation in cool combustible mixture. On reaching the detonation wave self-sustaining regime in its propagation in right hand side direction (Fig. 8, f) strong transverse waves degenerate into low amplitude oscillations of leading detonation front, which corresponds to cellular structure detected in experiments.

a) tube section 0 – 100 mm;

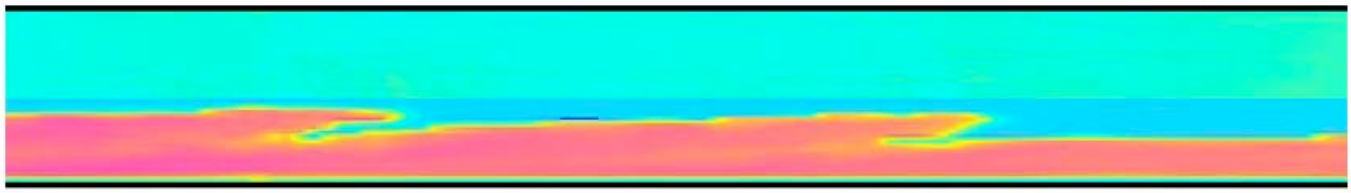

b) tube section 100 – 200 mm;

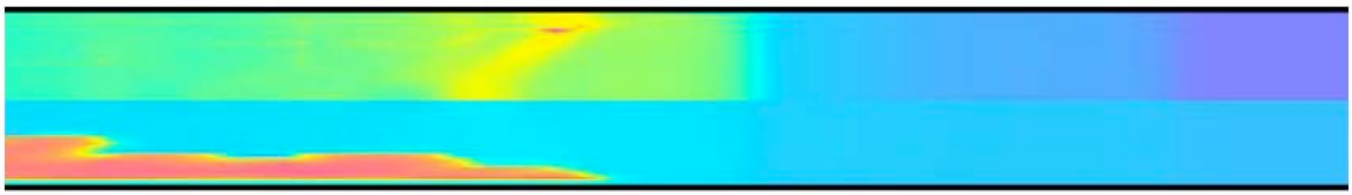

c) tube section 200 – 300 mm, time 0.5496 s;

d) tube section 200 – 300 mm, time 0.5763 s;

e) tube section 200 – 300 mm, time 0.6017 s;

f) tube section 300 – 400 mm, time 0.6017 s.

Fig. 8. Exposition of 100 mm length zones of the tube for different times. Mapping scale corresponds to that provided in Fig. 7.

Axial pressure profiles for successive stages of DDT process are shown in Fig. 9. The corresponding time moments for each curve are shown in the upper left hand side of the figure. The first two curves illustrate slow pressure increase in a weak shock wave overtaking flame zone. Then exothermal center (hot spot) appears which brings to an increase of pressure

behind leading shock wave. Fourth curve illustrates formation of an overdriven detonation, which on overtaking the leading shock enters cool combustible mixture (curves 5 and 6). Overdriven detonation gradually slows down to Chapman-Jouget mode. Both detonation and retonation waves have triangular profiles. Pressure in the zone of first explosion gradually decreases on detonation and retonation waves leaving the zone. On moving backward retonation wave has similar intensity as the detonation wave until it moves within the zone, wherein combustible mixture is still present near the axis (fifth curve in Fig 19). On entering reaction products occupying whole tube retonation wave degenerates in a shock wave, slows down and loses its intensity (sixth curve in Fig. 9).

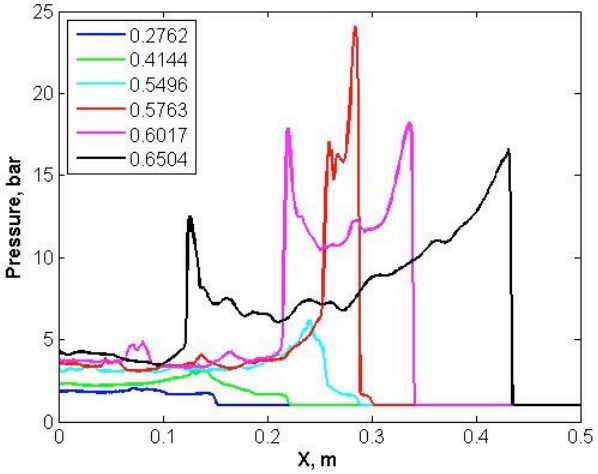

Fig. 9. Axial pressure profiles for successive time in DDT for hydrogen-air mixture $H_2 : O_2 : N_2 = 2:1:4$.

6 Conclusions

Predictive modeling 3-D code was developed making it possible to simulate chemically reacting turbulent pre-mixed and not pre-mixed flows. The code resolves hydrogen combustion chemistry in a sufficient way to model anomalous behavior of ignition delay times versus pressure. Within one and the same solver it was made possible to model establishing slow diffusion and kinetic combustion modes, as well as onset of detonation modes, and resolve deflagration to detonation transition nmechanisms. Verification and validation of the code were carried out.

In combustion chambers unsteady-state regime of establishing stable combustion was simulated: reagents burning process begins more like a diffusion flame near the injector nozzle, but more deep in the chamber chemical reaction becomes limiting factor and reaction rate begins to play important role as compared with diffusion. Under this condition reaction zone becomes wider and occupies the whole chamber.

Detonation degeneration and reestablishing on being transmitted from thin gap to a wide chamber was studied being relevant to pulse detonation engine functioning. It was demonstrated that on transmitting detonation from a narrow coaxial gap to a wide cylindrical chamber detonation wave degenerates but then could be reestablished due to cumulative energy effect in converging shock waves. While on transmitting expanding detonation waves from a narrow tube into a wide tube detonation wave has much more chances to degenerate for the same mixture compositions.

Deflagration to detonation transition process in hydrogen – air mixtures was simulated. After mild ignition shock wave in the gas is very weak in the beginning propagates far ahead of the slow flame front. Then turbulization of the mixture brings to an increase of flame propagation velocity, and the distance between flame zone and leading disturbance shortens. Flame propagates faster in the vicinity of the wall, where turbulence is stronger. Convergence of shock waves brings to pressure increase in the wall zone, which in the long run brings to formation of detonation and retonation waves propagating in the opposite directions. An overdriven detonation is formed, which on overtaking the leading shock enters cool combustible mixture. Overdriven detonation gradually slows down to Chapman-Jouget mode. Both detonation and retonation waves have triangular profiles. Pressure in the zone of first explosion gradually decreases on detonation and retonation waves leaving the zone. On moving backward retonation wave has similar intensity as the detonation wave until it moves within the zone, wherein combustible mixture is still present near the axis. On entering reaction products occupying whole tube retonation wave degenerates in a shock wave, slows down and loses its intensity.

Thus developed code makes it possible to simulate combustion phenomena relevant to propulsion applications and to study its peculiarities.

Acknowledgements:
The authors wish to acknowledge the support by Russian Foundation for Basic Research (Grant 13-03-00003) and Presidium of Russian Academy of Sciences (Program 18).

References:

[1] Smirnov N.N., Pushkin V.N., Dushin V.R., Kulchitskiy A.V. *Microgravity Investigation of Laminar Flame Propagation in Monodisperse Gas-Droplet Mixtures.* Acta Astronautica, 2007, vol. 61, 626-636.

[2] Betelin V.B., Smirnov N.N., Dushin V.R., Nikitin V.F., Kushnirenko A.G., Nerchenko V.A., Evaporation and ignition of droplets in combustion

chambers modeling and simulation, Acta Astronautica vol.70 (2012) pp. 23–35.
[3] V.R. Dushin, A.V. Kulchitskiy, V.A. Nerchenko, V.F. Nikitin, E.S. Osadchaya, Yu.G. Phylippov, N.N. Smirnov. *Mathematical Simulation For Non-Equilibrium Droplet Evaporation.* Acta Astronautica, 2008, vol. 63, pp 1360-1371.
[4] V.F. Nikitin, V.R. Dushin, Y.G. Phylippov, J.C. Legros. Pulse detonation engines: Technical approaches. //Acta Astronautica 64 (2009) 281–287.
[5] Smirnov N.N., Nikitin V.F., Unsteady-state turbulent diffusive combustion in confined volumes. Combustion and Flame, 1997, vol. 111, pp. 222-256.
[6] Smirnov N.N. and V.F.Nikitin, Comb. Exp. Shock Wave 40 (2):186-199, 2004.
[7] Smirnov N.N., Nikitin V.F., The Influence of Confinement Geometry on Deflagration to Detonation Transition in Gases. J. Phys. IV France, 12, Pr7, (2002) 341-351.
[8] N. N. Smirnov, V. F. Nikitin, S. Alyari Shurekhdeli. Investigation of Self-Sustaining Waves in Metastable Systems: Deflagration-to-Detonation Transition. JOURNAL OF PROPULSION AND POWER Vol. 25, No. 3, 2009 pp. 593-608.
[9] A. Liñán, M. Bollig, A.L. Sánchez, B. Lázaro. Reduced kinetic mechanisms for modelling LPP combustion gas turbines. RTO AVT Symposium on Gas Turbine Engine Combustion, Emissions and Alternative Fuels. Lisbon, Portugal, 1998; RTO MP-14.
[10] Peters, N., and Williams, F.A. Combustion and Flame, 68, 1987, p. 185.
[11] N.N. Smirnov, V.F. Nikitin Modeling and simulation of hydrogen combustion in engines. International Journal of Hydrogen Energy. (2014), vol. 39, Iss. 2, 1122-1136.
[12] Maas, U., and Warnatz, J. Ignition process in hydrogen-oxygen mixtures. Combustion and Flame, 74, No. 1, 1988, pp. 53-69.
[13] U. Maas, and S.B. Pope. Simplifying chemical kinetics: intrinsic low-dimensional manifolds in composition space. Combustion and Flame, 88, 239-264 (1992).
[14] V.V. Tyurenkova, N.N. Smirnov, V.M. Guendugov. Analytical solution for a single droplet diffusion combustion problem accounting for several chain reaction stages. Acta Astronautica 83 (2013) 208–215.
[15] R.J. Kee, J.A. Miller, and T.H. Jefferson. Chemkin: a general-purpose, problem-independent, transportable Fortran chemical kinetics code package. Sandia National Laboratories Report SAND80-8003 (1980).
[16] Gelfand B.E., Silnikov M.V., Medvedev S.P., Khomik S.V. Thermo- gas-dynamics of hydrogen combustion and explosion. St. Petersburg, Polytechnic Publ., 2009. (Гельфанд Б.Е., Сильников М.В., Медведев С.П., Хомик С.В. Термогазодинамика горения и взрыва водорода. – Санкт Петербург, Изд-во Политехн. Университета, 2009.)
[17] V.V.Tyurenkova Non-equilibrium diffusion combustion of a fuel droplet. Acta Astronautica 75 (2012) 78–84.
[18] Philip M. Dissertation “Experimentelle und theoretische Untersuchungen zum Stabilitatsverhalten von Drallflammen mit zentraler Ruckstromzone”. Karlsruhe University. 1991.
[19] V.B. Betelin, V.F. Nikitin, D.I. Altukhov, V.R. Dushin, Jaye Koo. Supercomputer modeling of hydrogen combustion in rocket engines. Acta Astronautica 89 (2013) 46–59
[20] Oppenheim, A.K., and Urtiew, P.A. "Experimental observations of the transition to detonation in an explosive gas," *Proceedings of the Royal Society, A295*, 1966, pp. 13-28.
[21] Salamandra, G.D. "On the interaction of a flame with a shock wave," *Physical Gas Dynamics*, USSR Academy of Sciences Publishes, 1959, pp. 163-167, in Russian.
[22] Bazhenova, T.V., and Soloukhin, R.I. "Gas ignition behind the shock waves," *Proceedings of the 7th International Symposium on Combustion*, Butterworths, London, 1959, pp. 866-875.
[23]Soloukhin, R.I. *Methods of measuring and main results of experiments in shock tubes*, Novosibirsk State University Publishes, Novosibirsk, Russia, 1969, in Russian.
[24]Smirnov, N.N., and Boichenko, A.P. "Transition of combustion to detonation in gasoline-air mixtures," *Combustion, Explosion and Shock Waves*, Vol. 22, No. 2, 1986, pp. 65-68.
[25] Smirnov, N.N., and Tyurnikov, M.V. "Experimental investigation of deflagration to detonation transition in hydrocarbon-air gaseous mixtures," *Combustion and Flame*, Vol. 100, Issue 4, 1995, pp. 661-668.
[26] Zeldovich, Ya. B., Librovich, V.B., Makhviladze, G.M., and Sivashinsky, G.I. "On the onset of detonation in a non-uniformly pre-heated gas," *Acta Astronautica*, Vol. 15, 1970, pp. 313-321.
[27] Merzhanov, A.G. "On critical conditions for thermal explosion of a hot spot," *Combustion and Flame*, Vol. 10, Issue 4, 1966, pp. 341-348.
[28] Borisov, A.A. “On the origin of the exothermic centers in gaseous mixtures,” *Acta Astronautica*, No. 1, 1974, pp. 909-920.
[29] Kailasanath, K., and Oran, E.S. "Ignition of flamelets behind incident shock waves and the transition to detonation," *Combustion Science and Technology*, Vol. 34, 1983, pp. 345-362
[30] Smirnov N.N., Panfilov I.I., Tyurnikov M.V., Berdyugin A.G. Dushin V.R., Presnyakov Yu.P. Theoretical and experimental investigation of

combustion to detonation transition in chemically active gas mixtures in closed vessels. Journal of Hazardous Materials, 1997, vol. 53, pp. 195-211.
[31]Brown, C.J., and Thomas G.O. "Experimental studies of shock-induced ignition and transition to detonation in ethylene and propane mixtures," *Combustion and Flame*, Vol. 117, Issue 4, 1999, pp. 861-870.
[32] Khohlov, A.M., and Oran E.S. "Numerical simulation of detonation initiation in a flame brush: the role of hot spots," *Combustion and Flame*, Vol. 119, Issue 4, 1999, pp. 400-416.
[33] Liberman M.A., Ivanov M.F., Kiverin A.D., Kuznetsov M.S., Chukalovsky A.A., Rakhimova T.V. Deflagration to detonation transition in highly reactive combustible mixture. Acta Astronautica, Vol. 67, iss. 7-8, (2010) pp. 688-701.
[34] Smirnov N.N., Nikitin V.F. Phylippov Yu.G. Deflagration to detonation transition in gases in tubes with cavities. Journal of Engineering Physics and Thermophysics, Vol. 83, No. 6, 2010, pp.1287-1316.
[35] V.B.Betelin, R.M.Shagaliev, S.V.Aksenov, I.M.Belyakov, Yu.N.Deryuguin, D.A.Korchazhkin, A.S.Kozelkov, V.F.Nikitin, A.V.Sarazov, D.K.Zelenskiy Mathematical simulation of hydrogen-oxygen combustion in rocket engines using LOGOS code. Acta Astronautica, Vol. 96, (2014) Pages 53–64.
[36] Smirnov N.N. Nikitin V.F. Khadem J. Aliari Shourekhdeli Sh. Onset of Detonation in Polydispersed Fuel-Air Mixtures. Proceedings of the Combustion Institute. 2007, vol. 31, pp. 832-841.
[37] Babkin V.S., Fast combustion of gases in the systems with hydraulic resistance. Combustion, Explosion, Shock Waves. (2012), vol. 48, No. 3, pp. 35-45.
[38] Bunev V.A., Babkin V.S. Numerical characteristics of the low-temperature oxidation of dimethyl ether with air. Mendeleev Commun.,2012, 22, C. 238-239.
[39] Meleeva O.V., Fomin N.A. Correlation analysis of digital images with sub-piksel precision. Optoelectronics, Instrumentation and data processing. (2012) Vol. 48, No 3, pp. 82-89.
[40] Gelfand B.E., Silnikov M.V., Chernyshov M.V. On the efficiency of semi-closed blast inhibitors. Shock Waves, (2010) vol. 20, No. 4, pp. 317-321.
[41] Khomik S.V., Veyssiere B., Medvedev S.P., Montassier V., Agafonov G.L., Silnikov M.V., On some conditions for detonation initiation downstream of a perforated plate. Shock Waves, (2013), 23 (3), pp. 207-211.